RESEARCH PAPER

OncoImmunology 1:4, 477–486; July 2012; © 2012 Landes Bioscience

Humanizing murine IgG3 anti-GD2 antibody m3F8 substantially improves antibody-dependent cell-mediated cytotoxicity while retaining targeting in vivo

Nai-Kong V. Cheung,* Hongfen Guo, Jian Hu, Dimiter V. Tassev and Irene Y. Cheung

Department of Pediatrics; Memorial Sloan-Kettering Cancer Center; New York, NY USA

Keywords: chimeric, humanized, monoclonal antibodies (MoAb), antibody-dependent cell-mediated cytotoxicity (ADCC), complement mediated cytotoxicity (CMC), peripheral blood mononuclear cells (PBMC), polymorphonuclear leukocytes (PMN)

Murine IgG3 anti-GD2 antibody m3F8 has shown anti-neuroblastoma activity in Phase I/II studies, where antibody-dependent cell-mediated cytotoxicity (ADCC) played a key role. Humanization of m3F8 should circumvent human anti-mouse antibody (HAMA) response and enhance its ADCC properties to reduce dosing and pain side effect. Chimeric 3F8 (ch3F8) and humanized 3F8 (hu3F8-IgG1 and hu3F8-IgG4) were produced and purified by protein A affinity chromatography. In vitro comparison was made with m3F8 and other anti-GD2 antibodies in binding, cytotoxicity, and cross-reactivity assays. In GD2 binding studies by SPR, ch3F8 and hu3F8 maintained K_D comparable to m3F8. Unlike other anti-GD2 antibodies, m3F8, ch3F8 and hu3F8 had substantially slower k_{off}. Similar to m3F8, both ch3F8 and hu3F8 inhibited tumor cell growth in vitro, while cross-reactivity with other gangliosides was comparable to that of m3F8. Both peripheral blood mononuclear cell (PBMC)-ADCC and polymorphonuclear leukocytes (PMN)-ADCC of ch3F8 and hu3F8-IgG1 were more potent than m3F8. This superiority was consistently observed in ADCC assays, irrespective of donors or NK-92MI-transfected human CD16 or CD32, whereas complement mediated cytotoxicity (CMC) was reduced. As expected, hu3F8-IgG4 had near absent PBMC-ADCC and CMC. Hu3F8 and m3F8 had similar tumor-to-non tumor ratios in biodistribution studies. Anti-tumor effect against neuroblastoma xenografts was better with hu3F8-IgG1 than m3F8. In conclusion, humanizing m3F8 produced next generation anti-GD2 antibodies with substantially more potent ADCC in vitro and anti-tumor activity in vivo. By leveraging ADCC over CMC, they may be clinically more effective, while minimizing pain and HAMA side effects. A Phase I trial using hu3F8-IgG1 is ongoing.

Introduction

Monoclonal antibody (MoAb) therapy is an accepted treatment modality for cancers, with five MoAb having received FDA approval for solid tumors in adults, including colorectal and breast cancer, non small cell lung cancer, squamous cell carcinoma and melanoma.[1,2] This modality, however, has remained inadequately exploited for the treatment of pediatric cancers. Unlike chemotherapy or radiation, MoAb is not myelosuppressive and genotoxic, generally with few long-term toxicities. These are critical considerations for young children. More importantly, MoAb is effective against metastatic cancer in blood, bone marrow and bone, typically found in high risk neuroblastoma (NB). As a class of agents, the pharmacokinetics and toxicities of human or humanized IgG1 antibodies have been extensively studied. In addition, antibodies can carry cytotoxic immune-based payloads, as well as radioisotopes, toxins or enzymes, thereby increasing the options for targeted therapy.

NB is the most common extracranial solid tumor of childhood. In ~50% of cases, curative strategies must tackle both soft tissue mass and metastases in the bone marrow (BM). Dose-intensive chemotherapy improves tumor resectability and post-surgical irradiation reduces the risk of relapse in the primary site to $< 10\%$.[3] However, BM disease, as evidenced by histology or metaiodobenzylguanidine (MIBG) scan, often persists and forebodes a lethal outcome.[4,5] In addition, osteomedullary relapse is common, despite achieving near complete remission after induction therapy. Attempts at treatment intensification have met with acute and long-term side effects, both of grave concern for young patients. There is a scarcity of promising new agents, and to date, few if any target/pathway-specific small molecules have shown major clinical benefit in patients with NB, although many promising leads continue to accumulate.[6] With a cure rate of $< 30\%$ at toxicity limits among Stage 4 patients diagnosed at ≥ 18 mo of age, there is substantial room for improvement.[7]

*Correspondence to: Nai-Kong V. Cheung; Email: cheungn@mskcc.org
Submitted: 02/27/12; Accepted: 03/01/12
http://dx.doi.org/10.4161/onci.19864

Ganglioside GD2 is an adhesion molecule abundant on NB. It is an ideal target for MoAb-based therapy in NB. Anti-GD2 MoAb mediates highly efficient antibody-dependent cell-mediated cytotoxicity (ADCC) of NB in the presence of human white cells. It also induces complement mediated cytotoxicity (CMC) of NB cells, which lack decay accelerating factor CD55[8] and homologous restriction factor CD59.[9] Complement deposition on NB cells enhances ADCC through activation of the iC3b receptor on neutrophils,[10,11] available even after dose-intensive or myeloablative chemotherapy plus stem cell transplant, provided colony stimulating factors are given.[12] Moreover, the use of intensive chemotherapy, which is standard of care for NB to achieve clinical remission, will result in prolonged lymphopenia and immunosuppression,[13] such that patients are less likely to reject murine or chimeric MoAb.[14]

At least two antibody families have been tested clinically, i.e., 3F8[15] and 14.18.[16] Chimeric (ch) 14.18 and 14.G2a were both derived from the variable region of murine MoAb 14.18.[17] They demonstrate ADCC and CMC of NB and melanoma cells in vivo.[18-21] Based on encouraging clinical responses in Phase I studies, ch14.18 was tested in large Phase II studies as consolidation therapy for Stage 4 NB (German NB90 and NB97 studies). For the 166 patients > 12 mo at diagnosis, even though event free survival was similar in patients receiving ch14.18 when compared with patients on maintenance chemotherapy, overall survival improved, and the rate of BM relapse was reduced.[22] In 2001, the Children's Oncology Group (COG) initiated a randomized Phase III trial to study the efficacy of the combination of ch14.18 with GM-CSF and IL-2 in preventing NB relapse in patients in complete remission after autologous stem cell transplant.[23] An interim analysis showed a statistically significant improvement in PFS and OS at 2 y.[24]

m3F8, a murine IgG3 MoAb specific for GD2, also induces cell death, and mediates efficient ADCC and CMC against NB in vitro.[15] Among patients with chemo-resistant marrow disease despite dose-intensive induction plus an aggressive salvage regimen, 80% achieved BM remission usually after 1 to 2 cycles of 5 days of m3F8 plus GM-CSF immunotherapy.[25] Given the activity of m3F8 against chemo-resistant marrow disease, its use was expanded to patients in their first remission with encouraging results.[26] These favorable clinical outcomes in children could be improved if 3F8 is given as maintenance therapy over the first 3–5 y of highest recurrence risk. However, human anti-mouse antibody (HAMA) is a limiting factor when the immune system recovers following cessation of chemotherapy. One strategy to reduce HAMA is to chimerize or humanize 3F8, which is the subject of this report.

Results

Amino acid sequences of chimeric-3F8 and humanized-3F8-IgG1/IgG4. The CDRs of the heavy and light chains of m3F8 were grafted onto human IgG1 frameworks based on their homology with human frameworks IGG HV3-33 and IGKV3-15, respectively. The amino acid sequences of chimeric and humanized heavy and light chains are shown in **Table 1** and **Table 2**, respectively. Additional constructs were made replacing the heavy chain sequences of m3F8 and hu3F8-IgG1 with the human IgG4 framework (**Table 3**), transfected into DG44 cells using the bluescript vectors. Both chimeric and humanized 3F8 were purified using standard protein A affinity chromatography.

On SDS gel, chimeric and humanized antibodies migrated as IgG with the appropriate size heavy and light chains; and by HPLC they all eluted as whole IgG with < 10% aggregate formation (data not shown). By ELISA they all bound to GD2 with similar avidity.

Binding kinetics by surface plasmon resonance (SPR). With antigen GD2 coated onto CM5 chips, kinetics of antibody

Table 1. Amino acid sequences of chimeric 3F8 heavy and light chains with CDR regions

Ch3F8 heavy chain-gamma1
QVQLKESGPGLVAPSQSLSITCTVSGFSVT**NYGVH**WVRQPPGKGLEWLG**VIWAGGITNYNSAFMS**RLSISKDNSKSQVFLKMNSLQIDDTAMYYCAS**RGGHYGYALDY** WGQGTSVTVSSASTKGPSVFPLAPSSKSTSGGTAALGCLVKDYFPEPVTVSWNSGALTSGVHTFPAVLQSSGLYSLSSVVTVPSSSLGTQTYICNVNHKPSNTKVDKRVEPKSCD KTHTCPPCPAPELLGGPSVFLFPPKPKDTLMISRTPEVTCVVVDVSHEDPEVKFNWYVDGVEVHNAKTKPREEQYNSTYRVVSVLTVLHQDWLNGKEYKCKVSNKALPAPIEKT ISKAKGQPREPQVYTLPPSRDELTKNQVSLTCLVKGFYPSDIAVEWESNGQPENNYKTTPPVLDSDGSFFLYSKLTVDKSRWQQGNVFSCSVMHEALHNHYTQKSLSLSPGK
Ch3F8 light chain-kappa
SIVMTQTPKFLLVSAGDRVTITC**KASQSVSNDVT**WYQQKAGQSPKLLIY**SASNRYS**GVPDRFTGSGYGTAFTFTISTVQAEDLAVYFC**QQDYSS**FGGGTKLEIKRTVAAPSVFI FPPSDEQLKSGTASVVCLLNNFYPREAKVQWKVDNALQSGNSQESVTEQDSKDSTYSLSSTLTLSKADYEKHKVYACEVTHQGLSSPVTKSFNRGEC

Table 2. Amino acid sequences of humanized 3F8 heavy and light chain with CDR regions

Hu3F8 heavy chain-gamma1
QVQLVESGPGVVQPGRSLRISCAVSGFSVT**NYGVH**WVRQPPGKGLEWLG**VIWAGGITNYNSAFMS**RLTISKDNSKNTVYLQMNSLRAEDTAMYYCAS**RGGHYGYALDY** WGQGTLVTVSSASTKGPSVFPLAPSSKSTSGGTAALGCLVKDYFPEPVTVSWNSGALTSGVHTFPAVLQSSGLYSLSSVVTVPSSSLGTQTYICNVNHKPSNTKVDKRVEPKSC DKTHTCPPCPAPELLGGPSVFLFPPKPKDTLMISRTPEVTCVVVDVSHEDPEVKFNWYVDGVEVHNAKTKPREEQYNSTYRVVSVLTVLHQDWLNGKEYKCKVSNKALPAPIEK TISKAKGQPREPQVYTLPPSRDELTKNQVSLTCLVKGFYPSDIAVEWESNGQPENNYKTTPPVLDSDGSFFLYSKLTVDKSRWQQGNVFSCSVMHEALHNHYTQKSLSLSPGK
Hu3F8 light chain-kappa
EIVMTQTPATLSVSAGERVTITC**KASQSVSNDVT**WYQQKPGQAPRLLIY**SASNRYS**GVPARFSGSGYGTEFTFTISSVQSEDFAVYFC**QQDYSS**FGQGTKLEIKRTVAAPS VFIFPPSDEQLKSGTASVVCLLNNFYPREAKVQWKVDNALQSGNSQESVTEQDSKDSTYSLSSTLTLSKADYEKHKVYACEVTHQGLSSPVTKSFNRGEC

Table 3. Amino acid sequences of chimeric and humanized 3F8 heavy chain of the IgG4 subclass with **CDR regions**

Ch3F8 heavy chain-gamma4
QVQLKESGPGLVAPSQSLSITCTVSGFSVT**NYGVH**WVRQPPGKGLEWLG**VIWAGGITNYNSAFMS**RLSISKDNSKSQVFLKMNSLQIDDTAMYYCAS**RGGHYGYALDY** WGQGTSVTVSSASTKGPSVFPLAPCSRSTSESTAALGCLVKDYFPEPVTVSWNSGALTSGVHTFPAVLQSSGLYSLSSVVTVPSSSLGTKTYTCNVDHKPSNTKVDKRVESKY GPPCPSCPAPEFLGGPSVFLFPPKPKDTLMISRTPEVTCVVVDVSQEDPEVQFNWYVDGVEVHNAKTKPREEQFNSTYRVVSVLTVLHQDWLNGKEYKCKVSNKGLPSSIEKT ISKAKGQPREPQVYTLPPSQEEMTKNQVSLTCLVKGFYPSDIAVEWESNGQPENNYKTTPPVLDSDGSFFLYSRLTVDKSRWQEGNVFSCSVMHEALHNHYTQKSLSLSLGK
Hu3F8 heavy chain-gamma4
QVQLVESGPGVVQPGRSLRISCAVSGFSVT**NYGVH**WVRQPPGKGLEWLG**VIWAGGITNYNSAFMS**RLTISKDNSKNTVYLQMNSLRAEDTAMYYCAS**RGGHYGYALDY** WGQGTLVTVSSASTKGPSVFPLAPCSRSTSESTAALGCLVKDYFPEPVTVSWNSGALTSGVHTFPAVLQSSGLYSLSSVVTVPSSSLGTKTYTCNVDHKPSNTKVDKRVESKYG PPCPSCPAPEFLGGPSVFLFPPKPKDTLMISRTPEVTCVVVDVSQEDPEVQFNWYVDGVEVHNAKTKPREEQFNSTYRVVSVLTVLHQDWLNGKEYKCKVSNKGLPSSIEKTIS KAKGQPREPQVYTLPPSQEEMTKNQVSLTCLVKGFYPSDIAVEWESNGQPENNYKTTPPVLDSDGSFFLYSRLTVDKSRWQEGNVFSCSVMHEALHNHYTQKSLSLSLGK

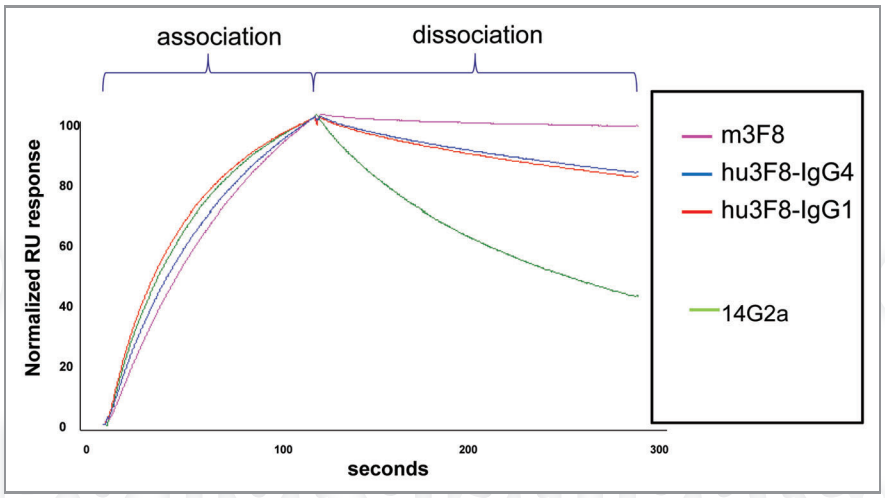

Figure 1. Comparative binding kinetics of anti-GD2 antibodies on solid phase GD2 when measured by surface plasmon resonance (Biacore T-100).

binding (k_{on}, k_{off} and KD) were compared by SPR using Biacore T-100. All engineered 3F8, including chimeric and humanized IgG1 and IgG4 had comparable k_{off} as m3F8, and better KD than other anti-GD2 antibody such as 14.G2a (**Fig. 1**) and ME36.1 (**Table 4**). The slow k_{off} of antibodies also translated into a slower wash-off when antibodies were reacted with GD2-positive tumor cells LAN-1 or M14 and then washed multiple times in wash buffer. With each wash, the remaining antibodies on the cell surface were detected using a secondary FITC-labeled goat anti-mouse antibody and mean fluorescent intensity determined by flow cytometry (data not shown).

Table 4. Binding kinetics of chimeric and humanized 3F8 by surface plasmon resonance

Antibody	k_{on}	k_{off}	KD (nM)
ch3F8-IgG1	1.15E + 05	1.45E − 03	13 ± 3
hu3F8-IgG1	9.19E + 04	1.03E − 03	11 ± 1
ch3F8-IgG4	9.40E + 04	1.28E − 03	14 ± 2
hu3F8-IgG4	1.18E + 05	1.76E − 03	15 ± 1
m3F8	1.74E + 05	8.74E − 04	5 ± 1
14.G2a	1.50E + 05	1.12E − 02	77 ± 8
ME36.1	1.21E + 05	2.79E − 03	19 ± 7

Low cross-reactivity with other gangliosides. In cross-reactivity studies, hu3F8-H1L1-IgG1 had similar profile as ch3F8-IgG1 and m3F8 (**Table 5**). There was low level of cross-reactivity with GD1b expressed as percent OD by ELISA relative to the OD on solid phase GD2. There was no cross-reactivity of m3F8, hu3F8 or 14.G2a with human N-CAM,[27] either by western blots or by SPR (data not shown).

Direct cytotoxicity. When these antibodies were added to neuroblastoma cells in vitro, they induced direct cell death and slowed down in vitro cell growth. Upon assayed by WST-8 in a 3-d culture system, m3F8 and hu3F8 had similar potency when their EC_{50}s were compared (**Table 6**). In contrast, 14.G2a was ~10-fold weaker in tumor cell killing.

Antibody potency in ADCC and CMC. Anti-GD2 antibodies were compared in ADCC assays using PBMC and PMN from volunteers as effectors and LAN-1 cells as targets. ADCC potencies of these antibodies were computed as the ratio (EC_{50} for 3F8)/(EC_{50} for MoAb) (**Table 7**). Relative to m3F8, ch3F8-IgG1 and hu3F8-IgG1 were ~300-fold stronger in PBMC-ADCC, and 18-fold stronger in PMN-ADCC. In addition, the maximal cytotoxicity achieved with both chimeric and humanized 3F8 of IgG1 subclass were substantially and consistently higher than that of m3F8 or 14.G2a, irrespective if it was PBMC-ADCC or PMN-ADCC.

Table 5. Low cross-reactivity with other gangliosides by ELISA (Mean ± SD)

Antibody	GM2/GD2	GD1a/GD2	GD1b/GD2	GT1b/GD2	GD3/GD2	GQ1b/GD2
ch3F8-IgG1	0%	0.2% ± 0.9%	8.8% ± 0.8%	0%	0.2% ± 0.9%	0%
hu3F8-IgG1	0%	0%	4.5% ± 0.7%	0%	0%	0%
ch3F8-IgG4	0%	0%	6.1% ± 2.2%	0%	0%	0%
hu3F8-IgG4	0%	0%	3.1% ± 1.6%	0%	0%	0%
m3F8	0%	0%	4.1% ± 1.0%	0%	0%	0%
14.G2a	0%	0%	0% ± 0.9%	0%	0%	0%

In order to examine the capability of MoAb in ADCC for individual FcR in the absence of inhibitory FcR, we tested ADCC using NK-92MI cells which do not carry human FcR on their cell surface. Upon transfection with human CD16 and CD32, they could mediate efficient ADCC. When these effector cells were used against LAN-1 targets, ch3F8-IgG1 and hu3F8-IgG1 was more efficient (> 10-fold) than m3F8 in CD16-ADCC, as well as CD32-ADCC. Hu3F8-IgG4 subclass antibodies had minimal PBMC-ADCC, PMN-ADCC, CD16-ADCC and CD32 activity when compared with m3F8. In human CMC, ch3F8, hu3F8 and 14G.2a were not as efficient as m3F8.

A representative panel of human NB cell lines was tested in cytotoxicity assays (CD16-ADCC, CD32-ADCC and CMC; **Table 8**). Even though most NB cell lines were sensitive, those with low GD2 antigen density (e.g., SKNJC2) were resistant. Overall, hu3F8 was generally much more efficient than m3F8 in cytotoxicity.

Targeting human neuroblastoma xenografts. Hu3F8-IgG1 and hu3F8-IgG4 were radiolabeled with ^{131}I. They all had comparable immunoreactivity of ~40–45% (data not shown). Their bio-distributions at 48 h were compared with that of ^{131}I-m3F8 in mice bearing sc LAN-1 xenografts. Tumor uptake when measured by %ID/gm was comparable between hu3F8-IgG1 (29.6%) and m3F8 (28.6%), nearly double that of hu3F8-IgG4 (**Table 9**). Tumor to non-tumor ratios was comparable among these four antibodies.

Treatment of neuroblastoma xenografts using 3F8 antibodies. LAN-1 is one of the most widely studied human NB cell lines. Even though the mouse effectors and mouse complement were generally suboptimal for testing monoclonal antibodies, it is the only established model for in vivo assays.[28] Mice xenografted with established human NB LAN-1 (0.5–1 cm diameter) were treated with iv m3F8 or hu3F8-IgG1 twice weekly for 4 weeks. Tumor size, weight, and survival were monitored. Hu3F8-IgG1 (100 μg dose) inhibited tumor growth significantly ($p < 0.05$), when compared with m3F8 (200 μg dose) or control mIgG3 (100 μg dose). At 20 μg dose, hu3F8-IgG1 was not effective (**Fig. 2**). Hu3F8-IgG1 (200 μg dose) was not more effective than hu3F8-IgG1 (100 μg dose) (data not shown). Survival of mice receiving 100–200 μg were significantly longer ($p = 0.003$) than mice receiving PBS control or m3F8 (data not shown).

Table 6. Direct cytotoxicity of neuroblastoma cell line LAN-1 in the presence of antibodies

Direct Cytotoxicity	
Antibody	**EC50 (ug/ml)**
ch3F8-IgG1	4.5 ± 1.2
hu3F8-IgG1	5.1 ± 1.2
ch3F8-IgG4	6.4 ± 1.8
hu3F8-IgG4	3.1 ± 0.0
m3F8	1.9 ± 0.2
14.G2a	47.1

Discussion

Anti-GD2 antibody is a proven therapy for GD2-postive NB.[29] Murine antibody 14.18 and its derivatives (14.G2a and ch14.18) have provided benchmarks for improving anti-GD2 therapy. We chose murine IgG3 antibody m3F8 for clinical development because of its 10-fold slower k_{off}, when compared with 14.G2a in GD2 binding kinetics by SPR. Among patients with chemo-resistant metastatic NB in the bone marrow, m3F8 plus GM-CSF induced 80% complete remissions,[30] and among patients with high risk metastatic NB in first remission, m3F8 plus GM-CSF was associated with > 75% overall long-term survival.[26] However, HAMA can diminish the effect of the murine antibody by neutralizing its ability to bind to its antigen, by blocking the direct effect of the antibody, and by accelerating the clearance of the antibody from circulation. Genetic engineering to change murine to human IgG frameworks should reduce the HAMA response. Ch14.18[31,32] and hu14.18[33] (both derived from the VH and VL of 14.G2a) have reduced immunogenicity in some but not all patients. We therefore tested the chimeric and humanized forms of 3F8 as potential next generation anti-GD2 antibodies

One criterion for successful chimerization and humanization is the preservation of affinity during genetic engineering. It was reassuring that a slow k_{off} in ch3F8 and hu3F8 was maintained.

Table 7. Antibody potency relative to m3F8 in ADCC and CMC against neuroblastoma LAN-1

Antibody	PBMC	PMN	NK-92MI-CD16	NK-92MI-CD32	CMC
ch3F8-IgG1	390	18	24	13	0.64
hu3F8-IgG1	217	19	12	15	0.40
ch3F8-IgG4	0	1	0	3	0.01
hu3F8-IgG4	0	4	0	1	0.03
m3F8	1	1	1	1	1
14.G2a	0.03	1	4	2	0.12

Table 8. Antibody potency relative to m3F8 in ADCC and CMC against seven neuroblastoma cell lines

	LAN1	NMB7	SKNLP	BE(1)N	SKNMM	SKNAS	SKNJC2
Antigen density/cell	499348	932191	541522	1080289	98613	33512	16089
Antibody				**ADCC-NK92-CD16**			
ch3F8-lgG1	33.7	47.6	34.5	47.1	52.7	93.0	no killing
hu3F8-lgG1	13.9	31.3	11.8	35.7	28.6	30.7	no killing
ch3F8-lgG4	0.0	0.0	0.0	0.0	0.0	0.0	no killing
hu3F8-lgG4	0.0	0.0	0.0	0.0	0.0	0.0	no killing
m3F8	1.0	1.0	1.0	1.0	1.0	1.0	no killing
14G2a	2.1	1.0	1.0	1.3	0.1	0.0	no killing
				ADCC-NK92-CD32			
ch3F8-lgG1	14.6	4.8	393.9	25.9	82.3	13.4	no killing
hu3F8-lgG1	15.1	7.4	1469.3	61.6	58.3	13.1	no killing
ch3F8-lgG4	1.0	0.8	3.7	1.0	1.3	0.5	no killing
hu3F8-lgG4	0.8	0.5	19.8	1.1	1.0	0.0	no killing
m3F8	1.0	1.0	1.0	1.0	1.0	1.0	no killing
14G2a	2.2	2.3	66.9	4.0	1.0	0.3	no killing
				CMC			
ch3F8-lgG1	0.74	0.19	0.24	0.15	0.08	0.07	no killing
hu3F8-lgG1	0.40	0.27	0.59	0.20	0.22	0.11	no killing
ch3F8-lgG4	0.03	0.00	0.00	0.00	0.00	0.00	no killing
hu3F8-lgG4	0.01	0.00	0.00	0.00	0.00	0.00	no killing
m3F8	1.00	1.00	1.00	1.00	1.00	1.00	no killing
14G2a	0.46	0.05	0.10	0.01	0.01	0.02	no killing

Table 9. Targeting of ^{131}I-labeled hu3F8 antibodies to LAN-1 xenografts in Biodistribution studies

LAN-1	% ID/gm						Tumor to non-tumor ratio					
	m3F8		hu3F8-lgG1		hu3F8-lgG4		m3F8		hu3F8-lgG1		hu3F8-lgG4	
N	**24**		**26**		**23**		**24**		**26**		**23**	
Organ	Mean	SEM	Mean	SEM	Mean	SEM	Mean	SEM	Mean	SEM	Mean	SEM
Adrenal	2.5	0.3	3.1	0.5	2.5	0.5	12	2	11	1	11	2
Bladder	2.5	0.3	3.1	0.4	1.9	0.3	11	1	10	1	10	1
Blood	4.2	0.6	4.4	0.7	3.7	0.6	8	1	7	1	7	1
Brain	0.2	0.0	0.2	0.0	0.1	0.0	187	19	132	10	125	10
Femur	0.8	0.1	1.2	0.1	0.7	0.1	35	4	24	2	27	3
Heart	1.7	0.2	2.2	0.3	1.6	0.2	18	2	13	1	12	1
Kidney	1.8	0.2	2.3	0.3	1.6	0.2	16	2	13	1	10	1
Large Int	1.0	0.1	1.6	0.2	0.8	0.1	29	4	18	2	22	3
Liver	2.2	0.2	3.0	0.4	1.7	0.3	13	1	10	1	10	1
Lung	2.9	0.4	3.5	0.5	2.4	0.3	11	1	8	1	7	1
Muscle	0.6	0.1	0.9	0.1	0.5	0.1	44	4	33	3	33	3
Skin	2.1	0.3	4.0	0.6	1.9	0.3	14	2	8	1	9	1
Small Int	0.7	0.1	1.1	0.1	0.5	0.1	39	4	26	3	30	3
Spine	1.0	0.1	1.4	0.2	0.9	0.1	27	2	21	2	21	2
Spleen	4.2	0.6	3.9	0.5	1.3	0.1	9	1	8	1	12	1
Stomach	1.5	0.2	2.4	0.2	1.4	0.2	21	2	12	1	13	2
Tumor	28.6	4.2	29.6	3.8	16.0	1.9	1	0	1	0	1	0

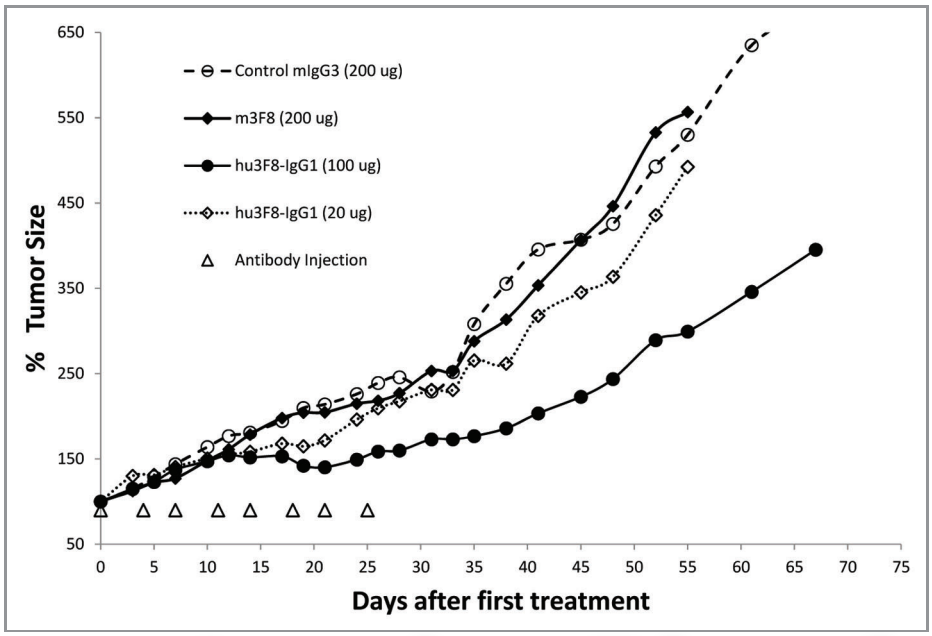

Figure 2. Treatment of LAN-1 subcutaneous neuroblastoma xenografts in athymic nude mice. Antibodies were administered intravenously twice weekly for a total of 8 doses. m3F8 and control mouse IgG3 had no effect on tumor growth. 100–200 ug of hu3F8-IgG1 had the strongest anti-tumor effect ($p < 0.05$, student t-test after day 21 of treatment), whereas such effect was substantially less if 20 ug was used.

But more importantly, the preservation and enhancement of in vitro effector function, as well as in vivo tumor targeting plus in vivo therapeutic properties could be critical. Both ch3F8-IgG1 and hu3F8-IgG1 showed > 200 fold more efficient PBMC-ADCC than m3F8, while PMN-ADCC was 19-fold. In sharp contrast, for CMC, ch3F8 and hu3F8 had substantially lower complement activating ability than m3F8.

This huge improvement in ADCC is most desirable, given recent evidence for its role in the anti-tumor effects of MoAb in patients. Among lymphoma patients treated with rituximab, both high affinity FcR2A and FcR3A were shown to have better response and survival advantage.[34] While the high affinity receptor FcR3A translated into < 10 improvement in ADCC in vitro,[35] overall response and time to progression improved by 200%.[34] When metastatic breast cancer was treated with Herceptin, patients with high affinity FcR3A had better overall response (83% vs. 35%, p = 0.03), and longer progression-free survival (p = 0.005).[36] For metastatic colorectal cancer treated with cetuximab, patients with low affinity FcR2A and FcR3A had comparable hazard ratios as patients with mutated *KRAS*.[37] Using m3F8, patients with the high affinity FcR3A receptor on myeloid cells were shown to have better survival.[38]

While binding affinity and effector functions are critical for therapeutic applications, cross-reactivity can pose unexpected toxicity issues. We showed that these chimeric and humanized forms for 3F8 had comparable cross-reactivity patterns as m3F8 both by ELISA assays with purified gangliosides, as well as by immunohistochemistry on a panel of normal human tissues (data not shown). Similar to m3F8, these engineered antibodies showed low level of reactivity to GD1b when compared with GD2. GD1b has been shown to be a highly prevalent ganglioside among NB tumors, especially when differentiated by retinoids.[39,40] This may be relevant, since 13-cis-retinoic acid is routinely given to patients undergoing immunotherapy for high risk NB. However, anti-GD1b antibodies have also been associated with sensory ataxic neuropathies.[41] Nevertheless, the safety profile of m3F8 with no permanent or late sensory neuropathies in more than 500 patients is reassuring.

CMC is unusually effective against human NB[42] because of its low expression of CD55[8] and CD59.[9] All anti-GD2 antibodies mediate efficient CMC, and m3F8 seems particularly effective. Yet, several studies with rituximab have suggested a negative role of complement activation in downregulating ADCC.[43] In clinical studies, higher activity of complement component C1qA was associated with less favorable response to rituximab therapy.[44] For anti-GD2 antibodies, complement activation was thought to be responsible for the pain side effects;[45] hence the Fc-CH2 domain mutated version (hu14.18K322A) is currently in clinical trial. Given these considerations, an overdrive of CMC is probably not desirable. It is reassuring that the increase in ADCC efficiency of both ch3F8 and hu3F8 were not accompanied by increased CMC.

In summary hu3F8 retains a slow k_{off}, allowing them to remain on tumor cell surface for longer periods. It mediates more potent ADCC in vitro and anti-tumor activity in vivo, while maintaining excellent targeting efficiency when compared with m3F8. By leveraging ADCC over CMC, hu3F8 treatment could potentially be made less painful, with reduced incidence or even avoidance of neutralizing antibodies. Preliminary results of the Phase I clinical trial of hu3F8 (Clinicaltrials.gov NCT01419834) have confirmed the low immunogenicity of hu3F8, with highly favorable pharmacokinetics.

Materials and Methods

Cell culture and human tissues. Human NB cell line LAN-1 was provided by Dr Robert Seeger (Children's Hospital of Los Angeles), and NB1691 by Dr Peter Houghton (St. Jude Children's Research Hospital). NK-92MI was obtained from American Type Culture Collection (ATCC). All cell lines were grown in F10 [RPMI 1640 medium supplemented with 10% fetal bovine serum (Hyclone, South Logan, UT), 2 mM glutamine, 100 U/ml penicillin, and 100 μg/ml streptomycin at 37°C in a 5% CO_2 incubator. Normal tissues as well as solid tumor samples of different histological types obtained at Memorial Sloan-Kettering Cancer Center (MSKCC) were snap-frozen in liquid nitrogen.

Monoclonal antibodies. m3F8 was a mouse IgG3 antibody with kappa light chain,[15] its anti-NB activity has been previously described.[15,46,47] It was produced as ascites and purified by affinity chromatography: protein A (GE Healthcare) with > 90% pure by SDS-PAGE. Anti-GD2 hybridoma ME36.1 was obtained from ATCC. 14.G2a was purchased from BD Biosciences.

Construction of the hu3F8-IgG1, hu3F8-IgG4, ch3F8-IgG1, and ch3F8-IgG4 antibody producer lines. Based on human homologs of m3F8, CDR sequences of both heavy and light chains of m3F8 were grafted into the human IgG1 framework and optimized. These hu3F8 genes were synthesized for CHO cells (Blue Heron Biotechnology or Genscript). Using the bluescript vector (Eureka, CA), these heavy and light chain genes of hu3F8 were transfected into DG44 cells and selected with G418 (InVitrogen, CA). Similarly, mouse VH and VL sequences were grafted onto human IgG1 and IgG4 frameworks to make the ch3F8-IgG1 and ch3F8-IgG4 recombinant antibodies. From two heavy chain and two light chain designs, four versions of hu3F8 genes were synthesized and expressed in DG44 cells. Based on in vitro stability, binding kinetics to GD2 by Biacore, and efficiency in ADCC, the final heavy and light chain sequences of hu3F8-IgG1 were chosen.

Purification of Hu3F8 and ch3F8. Hu3F8 and ch3F8 producer lines were cultured in Opticho serum free medium (InVitrogen) and the mature supernatant harvested. Protein A affinity column was pre-equilibrated with 25 mM sodium citrate buffer with 0.15 M NaCl, pH 8.2. Bound hu3F8 was eluted with 0.1 M citric acid/sodium citrate buffer, pH 3.9 and alkalinized (1:10 v/v ratio) in 25 mM sodium citrate, pH 8.5. It was passed through a Sartobind-Q membrane and concentrated to 5–10 mg/ml in 25 mM sodium citrate, 0.15 M NaCl, pH 8.2. Stability studies were performed on hu3F8-IgG1 in 25 mM sodium citrate 0.15 M NaCl pH 8.2 vs. PBS pH 7.4 in the presence or absence of 0.7 mg/ml of Tween 80 (Sigma). Two micrograms each of the proteins was analyzed by SDS-PAGE under non-reducing or reducing conditions using 4–15% Tris-Glycine Ready Gel System (Bio-Rad). Invitrogen SeeBlue Plus2 Pre-Stained Standard was used as the protein molecular weight marker. After electrophoresis, the gel was stained using PIERCE's GelCode Blue Stain Reagent. The gel was scanned using Bio-Rad Fluor-S MultiImager (Bio-Rad), and the band intensity quantified with Quantity One software (Bio-Rad).

Quantitation of hu3F8 and ch3F8 by ELISA. Microtiter plates were coated with GD2 at 20 ng per well. 150 μl per well of 0.5% BSA in PBS (diluent) was added to each plate for at least 30 min at ambient temperature to block excess binding sites. A purified batch of hu3F8-IgG1 was used to construct a standard curve starting at 0.5 μg/ml followed by 2-fold dilutions. 100 μl of standard and samples (also diluted 2-fold) were added to each well and incubated for 2.5 h at 37°C. After washing the plates with PBS, 100 μl of goat anti human-IgG (H^+L) (Jackson Research Laboratory) diluted at 1:3500 in diluent was added to each well and incubated for 1 h at 4°C. ELISA color reaction was developed with chromogen OPD (Sigma) with the substrate hydrogen peroxide for 30 min at room temperature (RT) in the dark. The reaction was stopped with 5N H_2S0_4 and the optical density (OD) read with ELISA plate reader MRX (Dynex) at 490 nm. Based on the standard curve, quantitation of hu3F8 and ch3F8 supernatants was calculated in micrograms/milliliters or micrograms/milligrams of protein.

In vitro binding kinetics by Biacore T-100 Biosensor (Biacore AB of GE Healthcare). CM5 sensor chip (Research grade) and related reagents were purchased from Biacore USA. The gangliosides GM1 was from ALEXIS Biochemicals (AXXORA L.L.C.), and GD2 from Advanced ImmunoChemical. In brief, gangliosides were directly immobilized onto the CM5 sensor chip via hydrophobic interaction.[48,49] Reference surface was immobilized with GM1. Active surface was immobilized with GD2 and GM1 in 1:1 ratio. Diluted mixture of GD2 and GM1 (50 μg/ml) was injected (300 μl) at a flow rate of 15 μl/min over 20 min. Extensive washing was followed with 10 mM NaOH (typically five washes of 20 μl at a flow rate of 5 μl /min) until a stable baseline was obtained.

Purified anti-GD2 MoAb were diluted in HBS-E buffer containing 250 mM NaCl at varying concentrations (50 ~1600 nM) prior to analysis. Samples (60 μl) were injected over the sensor surface at a flow rate of 30 μl/min over 2 min. Following completion of the association phase, dissociation was monitored in HBS-E buffer containing 250 mM NaCl for 300 sec at the same flow rate. At the end of each cycle, the surface was regenerated using 50 μl 20 mM NaOH at a flow rate of 50 μl/min over 1 min and 100 μl 4M $MgCl_2$ at a flow rate of 50 μl/min over 2 min. The biosensor curves obtained following injection of the samples over immobilized GD2 were subtracted with the control curves obtained with the samples injected over immobilized GM1 prior to kinetics analysis. The data were analyzed by the bivalent analyte model and default parameter setting for the rate constants using the Biacore T-100 evaluation software, and the apparent association on rate constant (k_{on}), dissociation off rate constant (k_{off}) and equilibrium dissociation constant (KD = k_{off}/k_{on}) were calculated.

ELISA for cross-reactivity with other gangliosides. GD2, GM2, GD1a, GD1b, GT1b, GD3, as well as GQ1b were coated on polyvinyl microtiter plates at 20 ng per well in 90% ethanol. Following air drying, wells were blocked with 0.5% BSA in PBS at 150 μl per well for 1 h at room temperature. Antibodies were added in triplicates at 1 μg/ml (100 μl per well) in 0.5% BSA. For background subtraction, wells with (1) no antigen and (2) no

sample were used. Following incubation for 2 h at 37°C and washing with PBS, HRP-goat anti-mouse IgG at 1:1000 dilution for mouse antibodies or HRP-goat anti-human IgG at 1:1000 dilution for humanized antibodies, all from Jackson Research Laboratory, were added. After incubation for 1 h at 4°C and further washing, color reaction was performed and OD was read using ELISA plate reader at 490 nm, and cross-reactivity expressed as % maximal binding to GD2.

Direct cytotoxicity. Antibodies were tested for their direct effect on tumor cell growth and survival in the absence of human serum or human effector cells. Tumor targets were dissociated with 2mM EDTA or Trypsin-EDTA, washed and plated onto 96-well flat bottom plates in F10 at 1.2×10^3 to 3.5×10^4 per well. After incubation for 24 h in a 5% CO_2 incubator at 37°C, increasing concentrations of antibodies in F10 are added to each well. Control wells received F10 alone. After incubation for 72 h at 37°C in 5% CO_2, WST-8 reagent (Cayman Chemical Co.). was added to each well and incubated in the dark in a CO_2 incubator at 37°C for 2–6 h. OD was read at 450 nm and 690 nm using ELISA plate reader. WST-8 assay was validated using direct cell counting using Trypan Blue (Sigma) or Beckman Coulter Counter (Beckman Coulter).

Antibody-dependent cell-mediated cytotoxicity (ADCC) by ^{51}Chromium Release. Target cells were detached with 2 mM EDTA in $Ca2^+$ $Mg2^+$ free PBS and washed in F10. Antigen density was estimated using Quantum Simply Cellular anti-Mouse IgG beads according the manufacturer's instructions (Bangs Laboratories, Inc.). For cytotoxicity assays, 100 μCi of ^{51}Cr was incubated with 10^6 target cells in a final volume of 250 μl and incubated for 1 h at 37°C with gentle resuspension of pellet at 15 min intervals. Cells were then washed and resuspended in 250 μl F10 and incubated for 30 min at 37°C. After washing, cells were counted and viability determined with Trypan Blue and quickly plated onto 96 well U-bottom plates. Peripheral blood from normal volunteers was collected into heparinized tubes. Blood was mixed with 3% dextran/PBS and kept at room temperature for 20 min to sediment the red cells. White cells were then ficolled and separated into peripheral blood mononuclear cells (PBMC) and polymorphonuclear leukocytes (PMN) for PBMC-ADCC and PMN-ADCC, respectively. Cells were washed in F10, counted and viability determined. PBMC-ADCC was done in the presence of 10 U/ml of IL-2 and PMN-ADCC in 2 ng/ml of GM-CSF. Antibodies were diluted in F10 from 1 μg/ml in 10-fold dilutions. Plates were incubated in a 37°C, 5% CO_2 incubator for 4 h. Released ^{51}Cr in the ADCC supernatant was collected for gamma counting. Total release was determined using 10% sodium dodecyl sulfate (SDS) and background spontaneous release was determined with F10 only without effectors. An effector:target (E:T) ratio of 50:1 was generally used. Similarly, ADCC assays were performed using NK-92MI cells stably transfected with the human CD16 or human CD32 Fc receptors. Unlike PBMC or PMN, no cytokines were needed in the assay. E:T ratio was generally kept at 20:1.

Biodistribution of MoAb in xenografted mice. Female athymic nude mice were purchased from Harlan Spraque Dawley, Inc. All procedures were performed in accordance with the protocols approved by our Institutional Animal Care and Use Committee and institutional guidelines for the proper and humane use of animals in research. LAN-1 tumor cells were harvested and resuspended in Matrigel (BD Biosciences). Cells ($2 \sim 10 \times 10^6$) were implanted subcutaneously (sc) to the flank of the mice in 0.1 ml volume using 22-gauge needles. Tumors were allowed to grow to the size of ~200 mm^3 before initiating treatment. Mice with established tumors were randomly separated into treatment groups. 100 μCi of radioiodinated antibody per mouse was injected intravenously and animals sacrificed usually at 48 h, and their organs removed and counted in a gamma counter (Packard Instruments, Perkin Elmer). These organs included skin, liver, spleen, kidney, adrenal, stomach, small intestine, large intestine, bladder, femur, muscle, tumor, heart, lung, spine, and brain. Based on the μCi accumulated in the organ and the organ weight, % injected dose (ID)/gm of mouse was calculated. Tumor to non-tumor ratios of % ID/gm was also calculated.

Therapy of LAN-1 neuroblastoma xenografts. Studies commenced when sc tumors reached ~200 mg. Mice were randomly assigned to treatment groups (n = 5). Antibodies were administered intravenously (iv) twice a week for a total of eight doses. Tumor volume and body weight were measured twice per week. Differences between tumor sizes were tested for significance by Student's t-test.

Disclosure of Potential Conflict of Interest

Hu3F8 patent was filed by Memorial Sloan-Kettering Cancer Center, and N.-K.C. was named as the inventor.

Acknowledgments

Supported in part by the Band of Parents Foundation and the Robert Steel Foundation. We thank Yi Feng and Hoa Tran for their excellent technical support.

References

1. Boyiadzis M, Foon KA. Approved monoclonal antibodies for cancer therapy. Expert Opin Biol Ther 2008; 8:1151-8; PMID:18613766; http://dx.doi.org/10.1517/14712598.8.8.1151
2. Yan L, Hsu K, Beckman RA. Antibody-based therapy for solid tumors. Cancer J 2008; 14:178-83; PMID:18536557; http://dx.doi.org/10.1097/PPO.0b013e318172d71a
3. Kushner BH, Wolden S, LaQuaglia MP, Kramer K, Verbel D, Heller G, et al. Hyperfractionated low-dose radiotherapy for high-risk neuroblastoma after intensive chemotherapy and surgery. J Clin Oncol 2001; 19:2821-8; PMID:11387353
4. Matthay KK, Edeline V, Lumbroso J, Tanguy ML, Asselain B, Zucker JM, et al. Correlation of early metastatic response by 123I-metaiodobenzylguanidine scintigraphy with overall response and event-free survival in stage IV neuroblastoma. J Clin Oncol 2003; 21:2486-91; PMID:12829667; http://dx.doi.org/10.1200/JCO.2003.09.122
5. Schmidt M, Simon T, Hero B, Schicha H, Berthold F. The prognostic impact of functional imaging with (123)I-mIBG in patients with stage 4 neuroblastoma >1 year of age on a high-risk treatment protocol: results of the German Neuroblastoma Trial NB97. Eur J Cancer 2008; 44:1552-8; PMID:18424129; http://dx.doi.org/10.1016/j.ejca.2008.03.013
6. Azarova AM, Gautam G, George RE. Emerging importance of ALK in neuroblastoma. Semin Cancer Biol 2011; 21:267-75; PMID:21945349; http://dx.doi.org/10.1016/j.semcancer.2011.09.005
7. Pearson AD, Pinkerton CR, Lewis IJ, Imeson J, Ellershaw C, Machin D, European Neuroblastoma Study Group & Children's Cancer and Leukaemia Group (CCLG formerly United Kingdom Children's Cancer Study Group). High-dose rapid and standard induction chemotherapy for patients aged over 1 year with stage 4 neuroblastoma: a randomised trial. Lancet Oncol 2008; 9:247-56; PMID:18308250; http://dx.doi.org/10.1016/S1470-2045(08)70069-X

8. Cheung NK, Walter EI, Smith-Mensah WH, Ratnoff WD, Tykocinski ML, Medof ME. Decay-accelerating factor protects human tumor cells from complement-mediated cytotoxicity in vitro. J Clin Invest 1988; 81:1122-8; PMID:2450893; http://dx.doi.org/10.1172/JCI113426
9. Chen S, Caragine T, Cheung NK, Tomlinson S. CD59 expressed on a tumor cell surface modulates decay-accelerating factor expression and enhances tumor growth in a rat model of human neuroblastoma. Cancer Res 2000; 60:3013-8; PMID:10850450
10. Kushner BH, Cheung NK. Absolute requirement of CD11/CD18 adhesion molecules, FcRII and the phosphatidylinositol-linked FcRIII for monoclonal antibody-mediated neutrophil antihuman tumor cytotoxicity. Blood 1992; 79:1484-90; PMID:1347707
11. Metelitsa LS, Gillies SD, Super M, Shimada H, Reynolds CP, Seeger RC. Antidisialoganglioside/granulocyte macrophage-colony-stimulating factor fusion protein facilitates neutrophil antibody-dependent cellular cytotoxicity and depends on FcgammaRII (CD32) and Mac-1 (CD11b/CD18) for enhanced effector cell adhesion and azurophil granule exocytosis. Blood 2002; 99:4166-73; PMID:12010822; http://dx.doi.org/10.1182/blood.V99.11.4166
12. Mackall CL. T-cell immunodeficiency following cytotoxic antineoplastic therapy: a review. Stem Cells 2000; 18:10-8; PMID:10661568; http://dx.doi.org/10.1634/stemcells.18-1-10
13. Mackall CL, Stein D, Fleisher TA, Brown MR, Hakim FT, Bare CV, et al. Prolonged CD4 depletion after sequential autologous peripheral blood progenitor cell infusions in children and young adults. Blood 2000; 96:754-62; PMID:10887145
14. Kushner BH, Cheung IY, Kramer K, Modak S, Cheung NK. High-dose cyclophosphamide inhibition of humoral immune response to murine monoclonal antibody 3F8 in neuroblastoma patients: broad implications for immunotherapy. Pediatr Blood Cancer 2007; 48:430-4; PMID:16421906; http://dx.doi.org/10.1002/pbc.20765
15. Cheung NK, Saarinen UM, Neely JE, Landmeier B, Donovan D, Coccia PF. Monoclonal antibodies to a glycolipid antigen on human neuroblastoma cells. Cancer Res 1985; 45:2642-9; PMID:2580625
16. Mujoo K, Kipps TJ, Yang HM, Cheresh DA, Wargalla U, Sander DJ, et al. Functional properties and effect on growth suppression of human neuroblastoma tumors by isotype switch variants of monoclonal antiganglioside GD2 antibody 14.18. Cancer Res 1989; 49:2857-61; PMID:2720646
17. Gillies SD, Lo KM, Wesolowski J. High-level expression of chimeric antibodies using adapted cDNA variable region cassettes. J Immunol Methods 1989; 125:191-202; PMID:2514231; http://dx.doi.org/10.1016/0022-1759(89)90093-8
18. Barker E, Mueller BM, Handgretinger R, Herter M, Yu AL, Reisfeld RA. Effect of a chimeric anti-ganglioside GD2 antibody on cell-mediated lysis of human neuroblastoma cells. Cancer Res 1991; 51:144-9; PMID:1988079
19. Barker E, Reisfeld RA. A mechanism for neutrophil-mediated lysis of human neuroblastoma cells. Cancer Res 1993; 53:362-7; PMID:8417829
20. Mueller BM, Reisfeld RA, Gillies SD. Serum half-life and tumor localization of a chimeric antibody deleted of the CH2 domain and directed against the disialoganglioside GD2. Proc Natl Acad Sci U S A 1990; 87:5702-5; PMID:2198570; http://dx.doi.org/10.1073/pnas.87.15.5702
21. Mueller BM, Romerdahl CA, Gillies SD, Reisfeld RA. Enhancement of antibody-dependent cytotoxicity with a chimeric anti-GD2 antibody. J Immunol 1990; 144:1382-6; PMID:2303711
22. Simon T, Hero B, Faldum A, Handgretinger R, Schrappe M, Niethammer D, et al. Consolidation treatment with chimeric anti-GD2-antibody ch14.18 in children older than 1 year with metastatic neuroblastoma. J Clin Oncol 2004; 22:3549-57; PMID:15337804; http://dx.doi.org/10.1200/JCO.2004.08.143
23. Gilman AL, Ozkaynak MF, Matthay KK, Krailo M, Yu AL, Gan J, et al. Phase I study of ch14.18 with granulocyte-macrophage colony-stimulating factor and interleukin-2 in children with neuroblastoma after autologous bone marrow transplantation or stem-cell rescue: a report from the Children's Oncology Group. J Clin Oncol 2009; 27:85-91; PMID:19047298; http://dx.doi.org/10.1200/JCO.2006.10.3564
24. Yu AL, Gilman AL, Ozkaynak MF, London WB, Kreissman SG, Chen HX, et al & Children's Oncology Group. Anti-GD2 antibody with GM-CSF, interleukin-2, and isotretinoin for neuroblastoma. N Engl J Med 2010; 363:1324-34; PMID:20879881; http://dx.doi.org/10.1056/NEJMoa0911123
25. Kushner B, Kramer K, Modak S, Cheung NK. Anti-GD2 anitbody 3F8 plus granulocyte-macrophage colony stimulating factor (GM-CSF) for primary refractory neuroblastoma (NB) in the bone marrow (BM). Proc Am Soc Clin Oncol 2007; 25:526s.
26. Cheung NK, Kushner BH, Kramer K, Modak S, Wolden S, LaQuaglia M. Anti-GD2 Murine Monoclonal Antibody (MoAb) 3F8 for Consolidation of First Complete/Very Good Partial Remission of High Risk Stage 4 Neuroblastoma (NB). Advances in Neuroblastoma Research (ANR). Stockholm, Sweden, 2010.
27. Patel K, Rossell RJ, Pemberton LF, Cheung NKV, Walsh FS, Moore SE, et al. Monoclonal antibody 3F8 recognises the neural cell adhesion molecule (NCAM) in addition to the ganglioside GD2. Br J Cancer 1989; 60:861-6; PMID:2481486; http://dx.doi.org/10.1038/bjc.1989.380
28. Bergman I, Basse PH, Barmada MA, Griffin JA, Cheung NK. Comparison of in vitro antibody-targeted cytotoxicity using mouse, rat and human effectors. Cancer Immunol Immunother 2000; 49:259-66; PMID:10941909; http://dx.doi.org/10.1007/s002620000120
29. Yu A, Gilman AL, Ozkaynak MF, London WB, Kreissman S, Chen HX, et al. A phase III randomized trial of the chimeric anti-GD2 antibody ch14.18 with GM-CSF and IL2 as immunotherapy following dose intensive chemotherapy for high-risk neuroblastoma: Children's Oncology Group (COG) study ANBL0032. J Clin Oncol 2009; 27:85-91; PMID:19047298
30. Kushner BH, Kramer K, Cheung NKV. Phase II trial of the anti-G(D2) monoclonal antibody 3F8 and granulocyte-macrophage colony-stimulating factor for neuroblastoma. J Clin Oncol 2001; 19:4189-94; PMID:11709561
31. Yu AL, Uttenreuther-Fischer MM, Huang CS, Tsui CC, Gillies SD, Reisfeld RA, et al. Phase I trial of a human-mouse chimeric anti-disialoganglioside monoclonal antibody ch14.18 in patients with refractory neuroblastoma and osteosarcoma. J Clin Oncol 1998; 16:2169-80; PMID:9626218
32. Ozkaynak MF, Sondel PM, Krailo MD, Gan J, Javorsky B, Reisfeld RA, et al. Phase I study of chimeric human/murine anti-ganglioside G(D2) monoclonal antibody (ch14.18) with granulocyte-macrophage colony-stimulating factor in children with neuroblastoma immediately after hematopoietic stem-cell transplantation: a Children's Cancer Group Study. J Clin Oncol 2000; 18:4077-85; PMID:11118469
33. Hank JA, Gan J, Ryu H, Ostendorf A, Stauder MC, Sternberg A, et al. Immunogenicity of the hu14.18-IL2 immunocytokine molecule in adults with melanoma and children with neuroblastoma. Clin Cancer Res 2009; 15:5923-30; PMID:19737959; http://dx.doi.org/10.1158/1078-0432.CCR-08-2963
34. Weng WK, Levy R. Two immunoglobulin G fragment C receptor polymorphisms independently predict response to rituximab in patients with follicular lymphoma. J Clin Oncol 2003; 21:3940-7; PMID:12975461; http://dx.doi.org/10.1200/JCO.2003.05.013
35. Niwa R, Hatanaka S, Shoji-Hosaka E, Sakurada M, Kobayashi Y, Uehara A, et al. Enhancement of the antibody-dependent cellular cytotoxicity of low-fucose IgG1 Is independent of FcgammaRIIIa functional polymorphism. Clin Cancer Res 2004; 10:6248-55; PMID:15448014; http://dx.doi.org/10.1158/1078-0432.CCR-04-0850
36. Musolino A, Naldi N, Bortesi B, Pezzuolo D, Capelletti M, Missale G, et al. Immunoglobulin G fragment C receptor polymorphisms and clinical efficacy of trastuzumab-based therapy in patients with HER-2/neu-positive metastatic breast cancer. J Clin Oncol 2008; 26:1789-96; PMID:18347005; http://dx.doi.org/10.1200/JCO.2007.14.8957
37. Bibeau F, Lopez-Crapez E, Di Fiore F, Thezenas S, Ychou M, Blanchard F, et al. Impact of FcgammaRIIa-FcgammaRIIIa polymorphisms and KRAS mutations on the clinical outcome of patients with metastatic colorectal cancer treated with cetuximab plus irinotecan. J Clin Oncol 2009; 27:1122-9; PMID:19164213; http://dx.doi.org/10.1200/JCO.2008.18.0463
38. Cheung NK, Sowers R, Vickers AJ, Cheung IY, Kushner BH, Gorlick R. FCGR2A polymorphism is correlated with clinical outcome after immunotherapy of neuroblastoma with anti-GD2 antibody and granulocyte macrophage colony-stimulating factor. J Clin Oncol 2006; 24:2885-90; PMID:16682723; http://dx.doi.org/10.1200/JCO.2005.04.6011
39. Hettmer S, McCarter R, Ladisch S, Kaucic K. Alterations in neuroblastoma ganglioside synthesis by induction of GD1b synthase by retinoic acid. Br J Cancer 2004; 91:389-97; PMID:15187999
40. Hettmer S, Malott C, Woods W, Ladisch S, Kaucic K. Biological stratification of human neuroblastoma by complex "B" pathway ganglioside expression. Cancer Res 2003; 63:7270-6; PMID:14612523
41. Gong Y, Tagawa Y, Lunn MP, Laroy W, Heffer-Lauc M, Li CY, et al. Localization of major gangliosides in the PNS: implications for immune neuropathies. Brain 2002; 125:2491-506; PMID:12390975; http://dx.doi.org/10.1093/brain/awf258
42. Saarinen UM, Coccia PF, Gerson S, Pelley R, Donovan D, Cheung NKV. In vitro eradication of neuroblastoma (NB) cells by monoclonal antibody (Mab) and human complement (C'): a method for purging autologous bone marrow (BM). Proc Am Assoc Cancer Res 1985; 26:291.
43. Wang SY, Veeramani S, Racila E, Cagley J, Fritzinger DC, Vogel CW, et al. Depletion of the C3 component of complement enhances the ability of rituximab-coated target cells to activate human NK cells and improves the efficacy of monoclonal antibody therapy in an in vivo model. Blood 2009; 114:5322-30; PMID:19805620; http://dx.doi.org/10.1182/blood-2009-01-200469

44. Racila E, Link BK, Weng WK, Witzig TE, Ansell S, Maurer MJ, et al. A polymorphism in the complement component C1qA correlates with prolonged response following rituximab therapy of follicular lymphoma. Clin Cancer Res 2008; 14:6697-703; PMID:18927313; http://dx.doi.org/10.1158/1078-0432.CCR-08-0745
45. Navid F, Santana VM, Barfield RC. Anti-GD2 antibody therapy for GD2-expressing tumors. Curr Cancer Drug Targets 2010; 10:200-9; PMID:20201786; http://dx.doi.org/10.2174/156800910791054167
46. Cheung NK, Modak S, Lin Y, Guo H, Zanzonico P, Chung J, et al. Single-chain Fv-streptavidin substantially improved therapeutic index in multistep targeting directed at disialoganglioside GD2. J Nucl Med 2004; 45:867-77; PMID:15136638
47. Modak S, Kramer K, Gultekin SH, Guo HF, Cheung NK. Monoclonal antibody 8H9 targets a novel cell surface antigen expressed by a wide spectrum of human solid tumors. Cancer Res 2001; 61:4048-54; PMID:11358824
48. Catimel B, Scott AM, Lee FT, Hanai N, Ritter G, Welt S, et al. Direct immobilization of gangliosides onto gold-carboxymethyldextran sensor surfaces by hydrophobic interaction: applications to antibody characterization. Glycobiology 1998; 8:927-38; PMID:9675226; http://dx.doi.org/10.1093/glycob/8.9.927
49. Hu J, Huang X, Ling CC, Bundle DR, Cheung NK. Reducing epitope spread during affinity maturation of an anti-ganglioside GD2 antibody. J Immunol 2009; 183:5748-55; PMID:19812201; http://dx.doi.org/10.4049/jimmunol.0901409